International Journal of Cardiology 413 (2024) 132399

Contents lists available at ScienceDirect

International Journal of Cardiology

journal homepage: www.elsevier.com/locate/ijcard

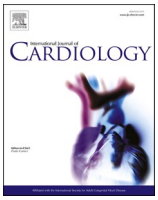

Lymphatic morphology and function in chronic right heart failure due to secondary tricuspid valve regurgitation☆

Benjamin Kelly [a,b,*], Lene Thorup [c], Niklas Telinius [b], Sheyanth Mohanakumar [b], Steffen Ringgaard [d,b], Steen H. Poulsen [e], Jesper K. Jensen [e], Vibeke E. Hjortdal [c]

[a] Department of Cardiothoracic Surgery, Aarhus University Hospital, Aarhus, Denmark.
[b] Department of Clinical Medicine, Aarhus University, Aarhus, Denmark
[c] The Heart Centre, Copenhagen University Hospital, Copenhagen, Denmark.
[d] The MR Research Centre, Aarhus University, Aarhus, Denmark.
[e] Department of Cardiology, Aarhus University Hospital, Aarhus, Denmark.

ARTICLE INFO

Keywords:
Heart failure
Tricuspid valve regurgitation
Lymph
Lymphatic imaging
Cardiovascular magnetic resonance imaging

ABSTRACT

Background: In heart failure, the capacity of the lymphatic system dictates symptoms of circulatory congestion. This study aimed at describing structural and functional changes of the lymphatic system in patients with chronic right-sided heart failure.

Methods: Individuals with long-standing severe tricuspid valve regurgitation and symptoms of heart failure were compared with age- gender- and weight-matched controls. Lymphatic structure and function were examined using non-contrast MR lymphangiography and near-infrared fluorescence imaging. Microvascular fluid dynamics and distribution were evaluated using strain gauge plethysmography and bio-impedance.

Results: In total nine patients and nine controls were included. Lymphatic morphology was unchanged in cases compared to controls with similar thoracic duct diameters 3.1(2.1–3.5) mm vs. 2.0(1.8–2.4) mm (p-value = 0.11), similar lymphatic classifications (p-value 0.34), and an identical number of lymphatic vessels in the legs 6 ± 1 vs. 6 ± 3 vessels/field (p-value = 0.72). Lymphatic function was comparable with contraction frequencies of 0.5 ± 0.2 and 0.5 ± 0.3 /min (p-value = 0.52) and a maximal lymphatic pumping pressure of 60 ± 13 and 57 ± 12 mmHg (p-value = 0.59) for cases and controls respectively. Finally, microvascular capillary filtration, isovolumetric threshold, and fluid distribution were similar between groups (p-value≥0.16 for all comparisons).

Conclusion: In this small exploratory study, individuals with severe secondary tricuspid valve regurgitation and right-sided heart failure displayed a largely similar lymphatic anatomy and function. Thoracic duct diameter displayed a trend towards increased size in the patient group. We speculate that cases were indeed stable and optimally treated at the time of examination, and with a lymphatic system largely unaffected by any of the current or prior hemodynamic changes.

1. Introduction

Heart failure is a leading cause of morbidity and mortality worldwide [1]. While declining cardiac function is central, circulatory congestion increases filtration of fluid to the interstitial space, producing many of the symptoms known to accompany heart failure. In tricuspid valve regurgitation (TR), a partial reversal of flow towards the right atrium and great veins causes venous congestion, ascites, and peripheral edema. Flowing into the interstitial space, the extravasated fluid represents increased work for the lymphatic system, working to maintain a

Abbreviations: TR, Tricuspid valve regurgitation; HFpEF, Heart failure with preserved ejection fraction; RHC, Right heart catheterization; NIRF imaging, Near-infrared fluorescent imaging; RAP, Right atrial pressure; CO, Cardiac output; VO_2, Oxygen consumption; A-VO_2diff, Arterial-venous O_2 difference; BSA, Body surface area; CI, Cardiac index; ICG, Indocyanine green.

☆ [1–5] All authors take responsibility for all aspects of the reliability and freedom from bias of the data presented and their discussed interpretations.

* Corresponding author at: Department of Cardiothoracic Surgery, Aarhus University Hospital, Aarhus, Denmark, Palle Juul-Jensens Boulevard 99, 8200 Aarhus N, Denmark.

E-mail address: benjaminkelly@clin.au.dk (B. Kelly).

https://doi.org/10.1016/j.ijcard.2024.132399
Received 2 April 2024; Received in revised form 11 June 2024; Accepted 25 July 2024
Available online 26 July 2024

healthy fluid equilibrium [2]. Multilayered smooth muscle cells and frequent valves, help the lymphatic vessels contract to propel fluid from the periphery back into the blood circulation [3,4]. Upon returning the lymphatic fluid, the congestion and higher venous pressure increase the afterload and the functional demands on the lymphatic vessels. In other entities of heart failure and animal models of TR, these changes are known to impact both lymphatic vessel morphology and function [5–10]. The interplay between heart failure, fluid accumulation, and the function of the lymphatic system has long been believed to play a central role in the pathophysiology of heart failure [11,12]. However, due to a scarcity of methods for evaluation of the lymphatic system, it remains largely undescribed [13].

This study aimed to use the state-of-the-art methods of non-contrast MR lymphangiography and near-infrared fluorescence (NIRF) imaging to describe central lymphatic morphology and peripheral lymphatic function in individuals with long-standing rate-regulated atrial fibrillation and chronic stable right-sided heart failure due to secondary severe TR.

2. Materials and methods

2.1. Study Design and Population

The study was conducted as an exploratory case-control study, examining the lymphatic function and morphology of patients with stable chronic right heart failure due to secondary severe TR compared to healthy age- and gender-matched controls. Patients followed at The Department of Cardiology, Aarhus University Hospital who had undergone echocardiography and right heart catheterization (RHC), were a minimum of 2 years post a diagnosis of TR, and with no changes in medication for the last two weeks, were invited to participate. Age- and gender-matched controls were recruited by online- and local community advertisements. All participants underwent a 5-h protocol containing lymphatic MRI, NIRF imaging of peripheral lymphatic function, bio-impedance measurements, and capillary filtration plethysmography.

The study was approved by the local committee on health and research ethics (1–10–72-113-20) and registered at www.clinicaltrials.gov (NCT04595448). Written informed consent was acquired from all study participants. The entire study was conducted in accordance with the Helsinki Declaration.

2.2. Echocardiographic assessment

Transthoracic echocardiography was performed using the GE VIVID E95 system (GE Medical System, Horten, Norway) with a 3.5-MHz transducer for 2-D evaluation. Cardiac chamber quantification was done following current guidelines [14]. All measurements were averaged over 4–6 consecutive heart cycles in end-expiration and the severe TR definition was based on current guidelines [15,16]. EchoPAC version 204 (GE-Vingmed Ultrasound, Horten, Norway) was used for image analysis.

2.3. Invasive hemodynamic assessment

RHC was conducted as previously described using a standard 7.5-F triple lumen Swan-Ganz thermistor and balloon-tipped catheter (Edwards Lifesciences, Irvine, CA, USA) [17]. During catheterization, an 8-french sheath was placed in the right internal jugular vein and a catheter advanced to the pulmonary artery. The catheter position was confirmed by distinct pressure waveforms and fluoroscopy. Systolic, diastolic, mean pulmonary artery pressure, mean right atrial pressure (RAP), pulmonary arterial wedge pressure, and CO were measured at rest. Oxygen consumption (VO_2) was measured with breath-by-breath analysis of each expiration (Jaeger Master Screen CPX, CareFusion, 234 GmbH, Hoechberg, Germany). The gas analyzer was calibrated before each test. The difference in systemic and pulmonary O_2 content (O_2 saturation x hemoglobin x 1.34) was used to estimate arterial-venous O_2 difference (A-VO_2diff), and the CO was calculated by direct Fick (CO = VO_2/A-VO_2diff) and indexed according to body surface area [18] (BSA) as cardiac index (CI).

2.4. Lymphatic MRI protocol

A T2-weighted MRI protocol for non-contrast lymphatic imaging was applied to visualize the central lymphatic anatomy of the neck, chest, and abdomen. In short; Images were obtained in the coronal orientation with a 3-T MRI system (Siemens Skyra; Siemens Healthineers, Germany). Coronal slices were acquired using a respiratory-gated (navigator) 3-dimensional fast T2-weighted fast spin-echo sequence with the following parameters: matrix, 448 × 448; voxel size, 0.9 × 0.9 × 0.8 mm3, field-of-view varied with body size and anatomic region, 100 to 400 cm2, repetition time, 2830 ms; echo time, 649 ms; no fat saturation; and no prepulse. This sequence was repeated twice for the desired coverage.

2.5. Lymphatic MRI analysis

Images were independently evaluated while blinded for outcomes. Measurements of thoracic duct diameter were performed at the terminal part of the thoracic duct in the left or right shoulder region, and at the level of the diaphragm. Furthermore, images were classified based on the anatomic location of prominent lymphatic channels within the neck and chest, images were graded on a scale from I-IV in accordance with a previously described lymphatic classification system [19,20]. The images were evaluated in the coronal plane only.

2.6. Near-infrared fluorescent imaging

Lymphatic vessels of the lower legs were investigated using a previously described custom-built NIRF imaging system [7,21,22]. Briefly, the system included a custom-designed 785 nm 450 mW laser (PowerTechnology), with a 780 ± 28-nm band-pass filter, which was used as the light source for the excitation of indocyanine green (ICG), and a lens was mounted to spread the light. Images were obtained with an electron-multiplier charge-coupled device camera (C9100–13; Hamamatsu, Japan), with a Navitar lens (25 mm f0.95) with two 835 ± 15 nm (>Optical Density 5) band-pass filters mounted in front and behind. Image capture was set to 3.33 Hz, and gain was set to 1200. ICG (DiagnosticGreen; Verdye, Denmark) was dissolved in sterile water and diluted with isotonic saltwater to a final concentration of 0.3 gL^{-1}, before injecting 0.1 mL (30 μg ICG) intradermally on three selected locations on each foot. Short sequences were filmed to confirm and visualize injections. Following a 15-min resting period to allow for acclimatization and the ICG to be taken up by the lymphatic vessels, five sequences were recorded (See video in supplementary material).

First, two 5-min baseline sequences of the superficial collecting lymphatic vessels on each lower leg were collected. To induce hyperthermia, capillary vessel dilatation, and increase extravasation of fluid i.e. production of lymph, one leg was placed in a container with 40-degree warm water for 5 min. Following hyperthermia, another 5-min sequence

was filmed. Then, the contralateral extremity underwent an exercise protocol consisting of 50 repetitions of calf contractions against resistance followed by another 5-min sequence. Finally, lymphatic pumping pressure was estimated by manually emptying lymphatic vessels and preventing lymphatic flow with a Hokanson sphygmomanometer cuff (Marcom Medical, Denmark) inflated to 80 mmHg using a Hokanson E20 Rapid cuff inflator (Hokanson AG101 air source, SC10 cuff; Marcom Medical). The pressure in the cuff was then reduced by 5 mmHg each fifth minute. The cuff pressure was noted at the time the lymphatic vessels were able to squeeze the fluorescent lymphatic fluid and the inflated cuff was noted as the pumping pressure.

2.7. Capillary Filtration Rate

A venous congestion protocol using a strain gauge plethysmograph setup (Hokanson EC6 and E20; Marcom Medical) was used to evaluate capillary filtration. Data were collected using LabChart 8 (ADinstruments). A 7-step, 25-min venous congestion protocol was used to measure capillary filtration. The cuff was rapidly inflated to and held at 20 mmHg, and the pressure was increased every 3 min with 10 mmHg until 80 mmHg was reached. The pressure applied to the cuff transmits to the veins inducing distension. Initially, tracings show a rapid increase due to the venous distension, followed by a linear plateau phase. When the capillary filtration, driven by the increasing hydrostatic pressure and modified by the capillary permeability, exceeds the capacity for lymphatic removal, the isovolumetric threshold, this plateau will display a linear increase.

The capillary filtration rate (μL × 100 mL^{-1} tissue×min^{-1}) was calculated as the averaged first derivative of the time-volume change (%) curve at steady state. These slopes are proportional to hydrostatic pressure by the microvascular filtration coefficient (μL × 100 mL of tissue–1 × min–1 × mm Hg–1). Strain gauge plethysmography force data (mN) were analyzed using LabChart 7 software (ADInstruments).

2.8. BioImpedance

Bioimpedance measurements were conducted with an ImpediMed SFB7 device (ImpediMed, Brisbane, Australia). Instrument calibration was checked before every use. Bioimpedance measurements provide the following estimations: Total body water, extracellular water, and intracellular water. Measurements were conducted three times, and the listed values represent the average.

2.9. Demographic, clinical, and hemodynamic data

For cases, medical records were retrospectively evaluated. Variables collected included: list of medications, functional class, lab results, latest echocardiographic evaluation, latest RHC, and recent hospitalizations. For healthy controls, all information was collected during the exam visit.

2.10. Statistical analysis

Continuous variables were presented as mean ± SD for normally distributed data and median (IQR) for non-normally distributed variables. Categorical variables were presented as n (%). Depending on the distribution, an unpaired *t*-test or Wilcoxon signed rank test was used when comparing the characteristics and outcomes of individuals in these groups. For categorical variables, Fisher's exact test was used to test for differences between groups. The intraclass correlation coefficient for a random effects model was used to check variability between raters on thoracic duct diameter and lymphatic contraction frequency. For all tests, a p-value <0.05 was considered statistically significant. All calculations were made using Stata v. 15.1 or GraphPad Prism v. 6.

3. Results

Eighteen individuals, nine patients, and nine healthy controls were included in the study. There was no difference between groups regarding age, gender, or BMI. All the patients with secondary severe TR were a minimum of 2 years post-diagnosis (defined as prescription of diuretics and symptoms). All were stable, with no recent changes in medication, weight, or manifestation of edema. Amongst the patients, all were classified as having atrial secondary tricuspid regurgitation [23] (A-STR) with the majority being due to atrial fibrillation (78%). All had a history of edema, and two had ongoing peripheral edema. None in the control group had peripheral edema or a history of it. For a detailed and individual description of cases, see Supplementary table 1.

3.1. Indices of cardiac volume and function

The median time from RHC and echocardiography to lymphatic examination was 4 (0–19) months and 7 (2–19) months respectively. Pressure measurements from RHC showed mildly increased RAP of 7 ± 2 mmHg. All remaining RHC parameters were within normal reference values. From the echocardiographic evaluation, individuals with TR had severe regurgitation with a median regurgitant volume of 51 mL (38–60). The right heart chambers were slightly dilated and right-heart function was normal. Indices of left heart volumes and function were largely within normal reference values (See Table 1).

3.2. Structural lymphatic evaluation

Thoracic duct diameter was measurable in eight cases and seven controls at inlet, and all cases and seven of controls at the level of the diaphragm. There was no difference in thoracic duct diameter at either location, although the diameter at the inlet showed a trend towards being more dilated in the TR group 3.1 mm vs. 2.0 mm (p-value = 0.11). Indexing thoracic duct diameter to BSA did not reveal any difference in thoracic duct diameter relative to size (p-value≥0.50 for both comparisons). Measurements of the thoracic duct by two independent raters displayed an ICC of 0.28 (−0.25–0.68), indicating poor correlation. Using a classification scheme for central lymphatic abnormalities, there was no difference in classification based on central lymphatic vessels. All cases and controls were scored as type 1 or 2, with no difference between distributions (p-value = 1.00) (Fig. 2). Looking at peripheral lymphatic vessels on both lower extremities, there was no difference in the number of vessels observed in cases and controls, 6 ± 1 and 6 ± 3 vessels/image respectively (p-value = 0.72).

3.3. Functional lymphatic evaluation

NIRF imaging was used to examine the function of the superficial lymphatic vessels of the lower extremities (See supplementary video). At baseline, there was no difference in the average lymphatic contraction frequency in cases or controls, 0.5 ± 0.2 and 0.5 ± 0.3 min-1 respectively (p-value = 0.52). The average maximal pressure generated by contractions of the lymphatic vessels was 60 ± 13 and 57 ± 12 mmHg (p-value = 0.59. After exposing the lymphatic vessels to hyperthermia and exercise, similar findings of no difference between groups were made (See Table 2). The ICC for analysis of the baseline NIRF sequences

Table 1
Demographics and Clinical Characteristics.

	Right heart failure ($n = 9$)	Controls (n = 9)
Age (years)	81 (74–82)	80 (73–82)
Female gender, n(%)	5 (56%)	7 (78%)
BMI (kg/m2)	25.9 (24–30.9)	25.1 (21.1–28.8)
BSA (m^2)	2.0 (1.8–2.1)	1.7 (1.6–1.8)
Mean arterial pressure (mmHg)	92 (86–102)	100 (96–101)
proBNP (ng/L)	637 (591–1800)	–
eGFR (mL/min)	57 (46–71)	
NYHA class (I/II/III/IV)	2/2/5/0	9/0/0/0
Hypertension, n(%)	5 (56%)	0 (0%)
Ischemic Heart Disease, n(%)	5 (56%)	0 (0%)
Diabetes, n(%)	2 (22%)	0 (0%)
NYHA class (I/II/III/IV)	2/2/5/0	9/0/0/0
Previous edema, n(%)	9 (100%)	0 (0%)
Current edema, n(%)	2 (22%)	0 (0%)
Medication n(%)		
Diuretics	9 (100%)	0 (0%)
Thiazide*	1 (11%)	0 (0%)
Loop**	8 (89%)	0 (0%)
Anticoagulation	8 (89%)	0 (0%)
DOAC	6 (67%)	0 (0%)
Vitamin K antagonist	1 (11%)	0 (0%)
Antiarrythmic agents	5 (56%)	0 (0%)
Betablocker	5 (56%)	0 (0%)
Amiodarone	1 (11%)	0 (0%)
Antidiabetic agents	2 (22%)	0 (0%)
Insulin	1 (11%)	0 (0%)
SGLT2 inhibitor	1 (11%)	0 (0%)
GLP-1 agonists	1 (11%)	0 (0%)
Right heart catheterization		
Mean right atrial pressure (mmHg)	7 ± 2	
Mean pulmonary artery pressure (mmHg)	18 (16–24)	
RV systolic pressure (mmHg)	31 (26–38)	
RV diastolic pressure (mmHg)	4 (3–6)	
Pulmonary capillary wedge pressure (mmHg)	9 (8–16)	
Transpulmonary gradient (mmHg)	7 (7–10)	
Cardiac output (L/min)	4.6 ± 0.6	
Cardiac index (L/kg/min)	1.9 (1.6–2.2)	
PVR (Wood units)	2.5 (1.3–2.9)	
Echocardiography		
Left ventricle		
Ejection fraction (%)	55 (51–60)	
End-diastolic volume indexed (mL/m2)	42 ± 7	
End-systolic volume indexed (mL/m2)	19 ± 3	
Left atrial volume (mL/m2)	44 ± 14	
Right ventricle		
Ejection fraction (%)	45 (38–53)	
End-diastolic volume indexed (mL/m2)	76 (45–81)	
End-systolic volume indexed (mL/m2)	35 (29–41)	
Tricuspid valve annulus (mm)	48 ± 5	
Tricuspid valve ERO (cm2)	0.6 (0.4–0.8)	
Tricuspid valve regurgitatin volume (mL)	51 (38–60)	
Tricuspid regurgitation (mild/moderate/severe)	0/0/9	
TAPSE (mm)	19 ± 4	
Right atrial volume (mL/m2)	73 ± 30	
Right ventricular strain - Free wall (%)	-22 ± 3	
Right ventricular strain - Global (%)	-19 ± 3	

Data presented as mean ± SD or median (IQR). Abreviations: BMI, Body mass index. BSA, Body surface area. NYHA, New York Heart Association. DOAC, Direct Oral Anticoagulants. PVR, Pulmonary vascular resistance. ERO, Effective regurgitant orifice. TAPSE, Tricuspid annular pulmonary systolic excursion. *1 x Centylmite 2.5 mg/day ** 1 x Burinex 2 g/day. 2 x Burinex 3 g/day. 2 x Furix 40 mg/day. 1 x Furix 80 mg/day. 2 x Furix 120 mg/day.

Table 2
Lymphatic and Microcirculatory Evaluation.

	Right heart failure	Controls	p-value
Near Infrared Fluorescent Imaging	**(n = 9)**	**(n = 9)**	
Peripheral structural and functional evaluation			
Number of superficial lymphatic vessels	6 ± 1	6 ± 3	0.72
Average contraction frequency (/min)	0.5 ± 0.2	0.5 ± 0.3	0.52
Contraction frequency after hyperthermia	0.8 (0.4–1.2)	0.5 (0.3–1.2)	0.39
Increase after hyperthermia	0.3 ± 0.3	0.4 ± 0.3	0.83
Contraction frequency after exercise	0.6 (0.5–0.7)	0.5 (0.3–0.8)	0.89
Increase after exercise	0.2 (−0.1–0.2)	0.1 (0–0.3)	0.86
Pumping pressure	60 ± 13	57 ± 12	0.59
Non-contrast MR lymphangiogram	**(n = 8)**	**(n = 7)**	
TD diameter inlet (mm)	3.1 (2.1–3.5)	2.0 (1.8–2.4)	0.11
TD diameter diaphragm (mm)	2.1 (1.9–2.4)	1.9 (1.7–2.3)	0.46
Classification of central abnormalities	**(n = 9)**	**(n = 9)**	
Normal/Type 1	7	8	1.00
Type 2	2	1	
Type 3	0	0	
Type 4	0	0	
Plethysmography - Venous congestion protocol	**(n = 7)**	**(n = 9)**	
Capillary filtration rate			
Isovolumetric threshold (mmHg)	33 (28–38)	36 (26–40)	0.96
Capillary filtration coefficient (μl × 100 mL of tissue–1 × min–1 × mm Hg–1)	4.4 (3.9–4.5)	4.1 (2.6–6.5)	0.16
Bioimpedance	**(n = 9)**	**(n = 9)**	
Fluid balance and distribution			
Total body water (%)	49.5 ± 7.3	50.0 ± 4.2	0.8
Extracellular fluid (% of total)	45.9 ± 5.0	44.9 ± 2.2	0.6
Intracellular fluid (% of total)	54.1 ± 5.0	55.1 ± 2.2	0.6

Data presented as mean ± SD or median (IQR). Abbreviations: MR Magnetic resonance, TD Thoracic duct.

showed substantial agreement with a value of 0.89 (0.69–0.96). The two individuals in the TR group displaying mild edema at the time of examination displayed lymphatic patterns of "dermal backflow" during examination.

3.4. Capillary filtration and fluid distribution

Applying strain gauge plethysmography and a bio impedance device, capillary filtration, isovolumetric threshold, and bodily fluid distribution were evaluated. Two measurements of capillary filtration were excluded during analysis due to artifacts that made analysis impossible. There was no difference in isovolumetric threshold between groups, 39 ± 13 and 37 ± 11 mmHg for cases and controls respectively (p-value = 0.76). Fluid distribution was similar with a total body water percentage of 50% for both groups (p-value = 0.8) and a similar distribution between the intracellular and extracellular space (p-value = 0.6 for both comparisons). (See Fig. 1.)

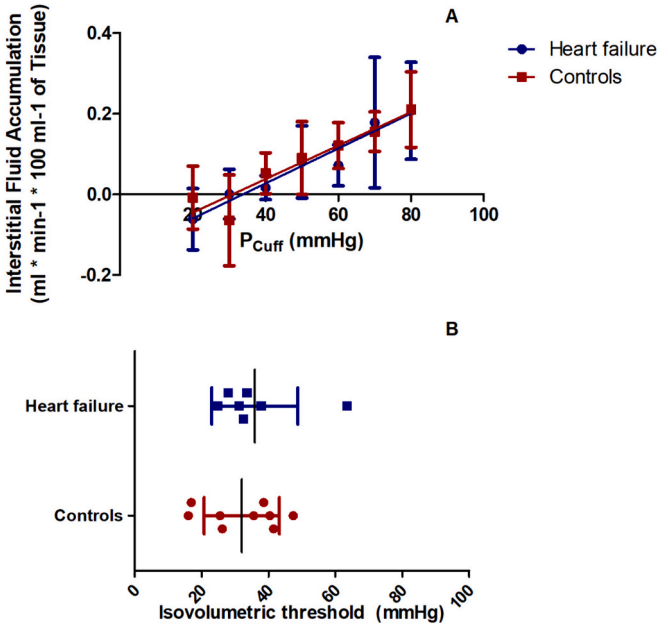

Fig. 1. Microvascular Fluid Dynamics. (A) Interstitial fluid accumulation at different hydrostatic pressures dictated by inflating a proximal cuff on the examined lower extremity to oppose venous drainage. Lines represent the overall best linear fit for heart failure group (blue) and healthy controls (red). The slope of the line is the microvascular coefficient of filtration.A greater slobe means a greater increase in the amount of fluid filtered to the interstitial space with each increase in pressure. (B) The intersect between the line of best fit and the x-axis is defined as the isovolumetric threshold. Here the forces favoring extravascular filtration exceed those opposing, and net fluid accumulation will start to develop. Data presented as mean ± SD; Pcuff = pressure applied to the cuff. (For interpretation of the references to colour in this figure legend, the reader is referred to the web version of this article.)

4. Discussion

In this small case-control study on lymphatic morphology and function in individuals with right-sided heart failure due to severe secondary TR, we report no anatomical changes in the central or superficial peripheral lymphatic anatomy and no changes in superficial peripheral lymphatic vessel function in the lower extremities. We speculate that cases were indeed well compensated from a cardiovascular perspective, as all received stable diuretic treatment at the time of investigation, exhibited only borderline elevated RAP, had estimations of total body water similar to healthy controls, and with only two cases displaying signs of mild peripheral edema.

The lymphatic vasculature is key in maintaining a healthy fluid equilibrium. Contrary to prior beliefs, venous reabsorption is negligible and all removal of fluid from the interstitial space is thus done by the lymphatic system [24]. Secondary TR caused by long-standing atrial fibrillation is a disease entity gaining an increased amount of attention due to continuous improvements in options of treatment [25,26]. Over time, the atrial fibrillation causes atrial enlargement leading to tricuspid annulus dilatation. A gradually progressing impairment of the valve coaptation then causes the development of secondary TR [26,27]. The accompanying redirection of flow from the right ventricle dually affects both hemodynamics and lymphodynamics. It increases RAP and CVP, further aggravating atrial and annulus dilatation, increasing regurgitation. From a lymphatic perspective, the increased CVP causes increased extravasation of fluid and interstitial edema, in addition to challenging the return of lymphatic fluid at the lymphovenous junctions. Overall, these individuals may be thought to have had years of gradually progressing TR with elevated RAP, venous congestion, and increased production of lymphatic fluid potentially affecting the lymphatic system. With this in mind, it is surprising that there were no observable differences in lymphatic vessel morphology or function in our study. However, the fact that all received treatment with diuretics and were stable at the time of examination may have mitigated any potential effects of

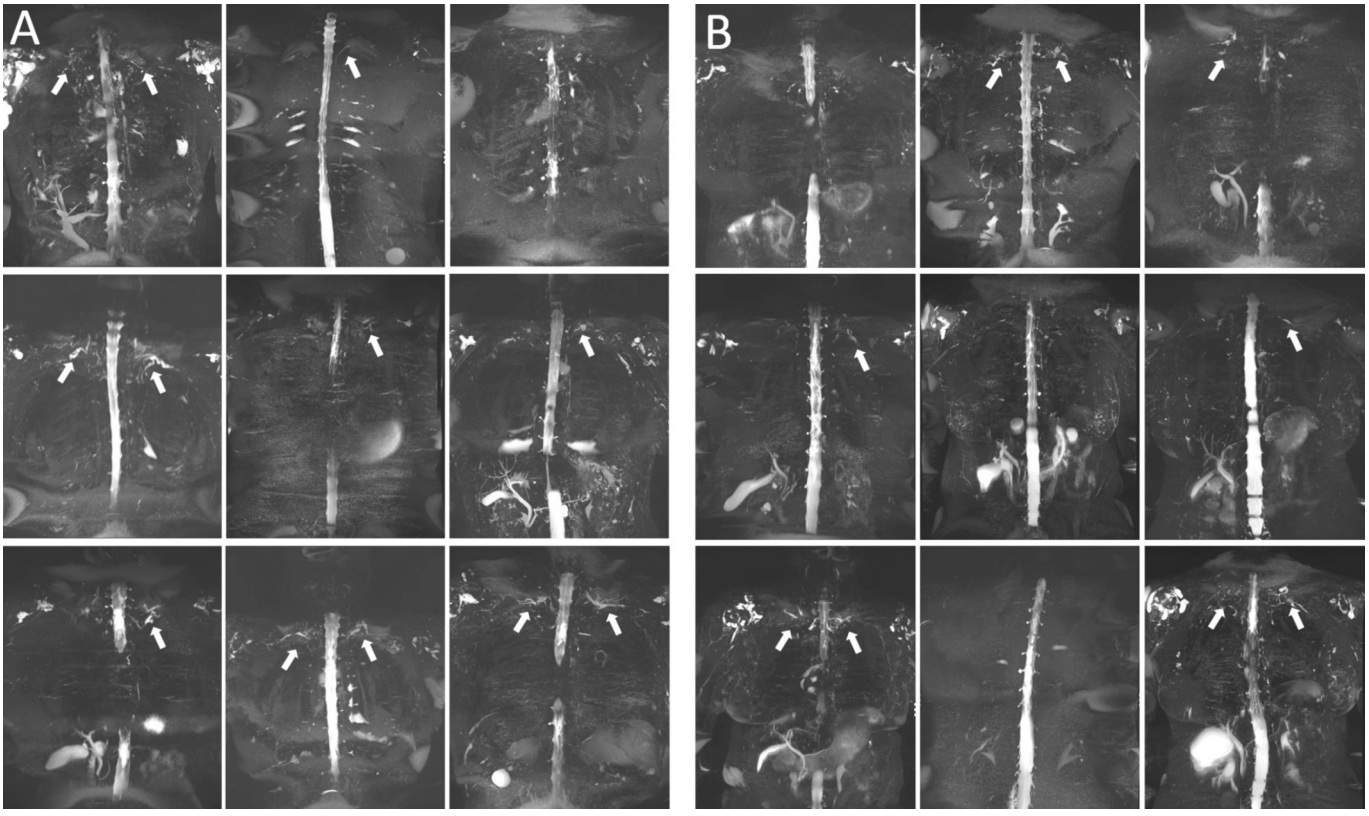

Fig. 2. Overview of the maximal intensity projection of non-contrast lymphatic imaging of healthy controls A) and individuals with stable chronic valve-related heart failure B). Central lymphatic vessels are marked with arrows. Additional lymphatic vessels may be visible in multi-slice images.

TR on the lymphatic system. It should be noted, that hemodynamic measurements were conducted at rest, an additional impact should be counted in during exercise as this is known to expose and aggravate the full hemodynamic impact of TR [28].

To the best of our knowledge, no studies have applied non-contrast MR lymphatic imaging to describe central lymphatic vessels in non-congenital heart failure. From other studies using ultrasound or thoracic duct cannulation, the thoracic duct is reported dilated in heart failure [8,29]. In an acute animal model of TR, thoracic duct dilatation, and lymphatic valve incompetence were shown to cause hepatic congestion and ascites, explaining some of the gap between hemodynamics and the clinical presentation [5]. In a similar but chronic model, TR was shown to increase central venous pressure and cause smooth muscle cell hypertrophy and dilation of the thoracic duct due to a combination of increased amounts of lymph fluid and increased afterload [6]. In congenital heart defects, central lymphatic morphology has been extensively studied. Here, findings of a dilated thoracic duct and central lymphatic abnormalities have been related to lymphatic complications and postoperative outcome [8,20,30,31,35]. In our study, we report no structural changes to the thoracic duct diameter and no abnormal lymphatic collaterals. Considering the sample size and the insecurity related to measurements of thoracic duct diameter, illustrated by the very poor intraclass correlation, larger studies are needed to test the tendency of a more dilated thoracic duct in the TR group. We imagine the initiation of diuretic treatment to have prevented irreversible dilation of the thoracic duct, or perhaps the magnitude of the increase was insufficient to cause lasting structural changes.

Regarding the structure and function of more peripheral lymphatic vessels, Rossitto et al. showed lymphatic signaling to be altered in individuals with HFpEF and reported a rarefaction of blood and lymphatic capillaries with an accompanying dilation of the later. In addition, the pressure threshold for fluid accumulation, i.e. the pressure at which capillary filtration exceeded the lymphatic removal of interstitial fluid was significantly lower in the heart failure group, causing authors to report a reduced lymphatic reserve in this population. In the current study, NIRF imaging was used to visualize and examine the superficial collecting lymphatic vessels of the lower extremities. We found no changes in the number of larger lymphatic vessels, which aligns with the similar levels of podoplanin between groups, a glycoprotein found in larger lymphatic vessels, also reported by Rossitto et al. [10] Although our population is largely considered a subtype of HFpEF, with a comparable distribution of age, gender, preserved left ventricular function, diabetes and venous pressures it is unknown if the same degree of inflammation and microvascular dysfunction previously observed [10] is also present in our specific subgroup.

As a first, we report the peripheral lymphatic function in individuals with compensated right heart failure due to secondary TR to be similar to that of age-matched and heart-healthy controls. Although in contradiction with our initial hypothesis, the findings of similar fluid distributions on bio impedance and normal RAPs underline the fact that these individuals are indeed well compensated, have a comparable fluid balance, and have an unaffected lymphatic function both at rest and when stressed by exercise and hyperthermia. In a recent study, Ponikowska et al. applied NIRF lymphography to evaluate lymphatic removal from the lower extremities in individuals with acute or chronic heart failure compared to healthy controls. The chronic heart failure group, aligning with our findings, displayed lymphatic removal similar to that of healthy controls while the acute decompensated heart failure group displayed fast and significant lymphatic removal in the majority of cases [32]. Combined with our findings, these studies are novel and warrant further examination. As a curiosity, the two individuals displaying peripheral edema at the time of examination also displayed patterns of lymphatic dermal backflow on NIRF. Lymphatic dermal backflow relates to the development of edema [33], and suggests the cause of edema in the two cases to be a local structural change leading to reduced lymphatic removal rather than excessive filtration and extravasation of fluid. Adding to the findings of no difference, the isovolumetric threshold during a venous congestion strain gauge plethysmography protocol was similar, indicating unchanged lymphatic reserve and an unaffected microcirculation and capillary integrity. All findings suggest that fluid homeostasis and lymphatic function remain unaffected in right-heart failure due to TR when appropriate diuretic treatment is provided. With device-mediated decongestive therapy aimed at improving lymphatic return being trialed in humans with acute-on-chronic heart failure, an improved understanding of lymphatic function in different types of heart failure remains relevant and may assist in qualifying patient selection [34].

4.1. Limitations

Although applying an extensive protocol for structural and functional lymphatic examination, the number of participants was limited. The inclusion criteria led to a rather specific study population with severe secondary TR, well-treated and clinically stable at the time of evaluation. All individuals were exposed to varying degrees of TR over multiple years. However, the exact duration and magnitude of the venous congestion transduced to the lymphatic system is unknown. In addition, the time between echocardiography, right-heart catheterization, and lymphatic evaluation was variable, and reported findings from echocardiography and right-heart catheterization may not reflect the exact hemodynamics at the time of lymphatic evaluation. For future studies, examining the peripheral lymphatic function and capillary filtration of individuals with untreated, uncompensated heart failure or individuals before and after initiation of diuretic treatment would be of great interest.

5. Conclusion

In this case-control study on lymphatic function and morphology in individuals with chronic right-heart failure due to severe secondary TR, we report no changes in the central or peripheral lymphatic anatomy and no changes in peripheral lymphatic function in the lower extremities. We speculate that cases were indeed stable and optimally treated at the time of examination, and with a lymphatic system unaffected by any of the current or prior hemodynamic changes. An understanding of the differences in lymphatic function in chronic and acute decompensated heart failure is still warranted.

Funding statement

BK carried out the work for this study, while funded by a scholarship from Aarhus University.

VEH is the recipient of a grant from the Novo Nordic Foundation (NNF23OC0082100).

Ethics approval and patient consent

The study was approved by the local committee on health and research ethics (1–10–72-113-20) and registered at www.clinicaltrials.gov (NCT04595448). Written informed consent was acquired from all study participants. The entire study was conducted in accordance with the Helsinki Declaration.

CRediT authorship contribution statement

Benjamin Kelly: Writing – review & editing, Writing – original draft, Visualization, Validation, Software, Resources, Project administration, Methodology, Investigation, Formal analysis, Data curation, Conceptualization. **Lene Thorup:** Writing – review & editing, Writing – original draft, Formal analysis. **Niklas Telinius:** Writing – review & editing, Writing – original draft, Visualization, Validation, Formal analysis, Data curation. **Sheyanth Mohanakumar:** Writing – review &

editing, Writing – original draft, Visualization, Formal analysis, Data curation, Conceptualization. **Steffen Ringgaard:** Writing – review & editing, Resources, Investigation, Data curation, Conceptualization. **Steen H. Poulsen:** Writing – review & editing, Supervision, Investigation, Data curation, Conceptualization. **Jesper K. Jensen:** Writing – review & editing, Supervision, Resources, Methodology, Investigation, Formal analysis, Data curation, Conceptualization. **Vibeke E. Hjortdal:** Writing – review & editing, Visualization, Supervision, Resources, Methodology, Funding acquisition, Formal analysis, Conceptualization.

Declaration of competing interest

The authors report no relationships that could be construed as a conflict of interest.

Data availability

All data will be made available from the corresponding author on reasonable request.

Appendix A. Supplementary data

Supplementary data to this article can be found online at https://doi.org/10.1016/j.ijcard.2024.132399.

References

[1] A.P. Ambrosy, G.C. Fonarow, J. Butler, O. Chioncel, S.J. Greene, M. Vaduganathan, S. Nodari, C.S.P. Lam, N. Sato, A.N. Shah, M. Gheorghiade, The global health and economic burden of hospitalizations for heart failure: lessons learned from hospitalized heart failure registries, J. Am. Coll. Cardiol. 63 (2014) 1123–1133.

[2] J.W. Breslin, Y. Yang, J.P. Scallan, R.S. Sweat, S.P. Adderley, W.L. Murfee, Lymphatic vessel network structure and physiology, Compr. Physiol. 9 (2018) 207–299.

[3] J.W. Breslin, Mechanical forces and lymphatic transport, Microvasc. Res. 96 (2014) 46–54.

[4] J.P. Scallan, S.D. Zawieja, J.A. Castorena-Gonzalez, M.J. Davis, Lymphatic pumping: mechanics, mechanisms and malfunction, J. Physiol. 594 (2016) 5749–5768.

[5] Y. Dori, J. Mazurek, E. Birati, C. Smith, Ascites in animals with right heart failure: correlation with lymphatic dysfunction, J. Am. Heart Assoc. 12 (2023) e026984.

[6] X. Lu, M. Wang, L. Han, J. Krieger, J. Ivers, S. Chambers, M. Itkin, D. Burkhoff, G. S. Kassab, Changes of thoracic duct flow and morphology in an animal model of elevated central venous pressure, Front. Physiol. 13 (2022) 798284.

[7] S. Mohanakumar, N. Telinius, B. Kelly, H. Lauridsen, D. Boedtkjer, M. Pedersen, M. de Leval, V. Hjortdal, Morphology and function of the lymphatic vasculature in patients with a Fontan circulation, Circ. Cardiovasc. Imaging 12 (2019) e008074.

[8] Y. Dori, M.S. Keller, M.A. Fogel, J.J. Rome, K.K. Whitehead, M.A. Harris, M. Itkin, MRI of lymphatic abnormalities after functional single-ventricle palliation surgery, AJR Am. J. Roentgenol. 203 (2014) 426–431.

[9] J.J. Savla, B. Kelly, E. Krogh, C.L. Smith, G. Krishnamurthy, A.C. Glatz, A. G. DeWitt, E.M. Pinto, C. Ravishankar, M.J. Gillespie, M.L. O'Byrne, F.A. Escobar, J.J. Rome, V. Hjortdal, Y. Dori, Occlusion pressure of the thoracic duct in Fontan patients with lymphatic failure: does dilatation challenge contractility? World J Pediatr Congenit Heart Surg. 13 (2022) 737–744.

[10] G. Rossitto, S. Mary, C. McAllister, K.B. Neves, L. Haddow, J.P. Rocchiccioli, N. N. Lang, C.L. Murphy, R.M. Touyz, M.C. Petrie, C. Delles, Reduced lymphatic Reserve in Heart Failure with Preserved Ejection Fraction, J. Am. Coll. Cardiol. 76 (2020) 2817–2829.

[11] M. Itkin, S.G. Rockson, D. Burkhoff, Pathophysiology of the lymphatic system in patients with heart failure: JACC state-of-the-art review, J. Am. Coll. Cardiol. 78 (2021) 278–290.

[12] M. Fudim, H.M. Salah, J. Sathananthan, M. Bernier, W. Pabon-Ramos, R. S. Schwartz, J. Rodés-Cabau, F. Côté, A. Khalifa, S.A. Virani, M.R. Patel, Lymphatic dysregulation in patients with heart failure: JACC review topic of the week, J. Am. Coll. Cardiol. 78 (2021) 66–76.

[13] P. Houck, H. Dandapantula, E. Hardegree, J. Massey, Why we fail at heart failure: lymphatic insufficiency is disregarded, Cureus 12 (2020) e8930.

[14] R.M. Lang, L.P. Badano, V. Mor-Avi, J. Afilalo, A. Armstrong, L. Ernande, F. A. Flachskampf, E. Foster, S.A. Goldstein, T. Kuznetsova, P. Lancellotti, D. Muraru, M.H. Picard, E.R. Rietzschel, L. Rudski, K.T. Spencer, W. Tsang, J.U. Voigt, Recommendations for cardiac chamber quantification by echocardiography in adults: an update from the American Society of Echocardiography and the European Association of Cardiovascular Imaging, Eur. Heart J. Cardiovasc. Imaging 16 (2015) 233–270.

[15] R.T. Hahn, State-of-the-art review of echocardiographic imaging in the evaluation and treatment of functional tricuspid regurgitation, Circ. Cardiovasc. Imaging (2016) 9.

[16] W.A. Zoghbi, D. Adams, R.O. Bonow, M. Enriquez-Sarano, E. Foster, P.A. Grayburn, R.T. Hahn, Y. Han, J. Hung, R.M. Lang, S.H. Little, D.J. Shah, S. Shernan, P. Thavendiranathan, J.D. Thomas, N.J. Weissman, Recommendations for noninvasive evaluation of native Valvular regurgitation: a report from the American Society of Echocardiography developed in collaboration with the Society for Cardiovascular Magnetic Resonance, J. Am. Soc. Echocardiogr. 30 (2017) 303–371.

[17] J.K. Jensen, T.S. Clemmensen, C.A. Frederiksen, J. Schofer, M.J. Andersen, S. H. Poulsen, Clinical performance and exercise hemodynamics in patients with severe secondary tricuspid regurgitation and chronic atrial fibrillation, BMC Cardiovasc. Disord. 21 (2021) 276.

[18] D. Du Bois, E.F. Du Bois, A formula to estimate the approximate surface area if height and weight be known. 1916, Nutrition 5 (1989) 303–311 (discussion 312-3).

[19] R.M. Ghosh, H.M. Griffis, A.C. Glatz, J.J. Rome, C.L. Smith, M.J. Gillespie, K. K. Whitehead, M.L. O'Byrne, D.M. Biko, C. Ravishankar, A.G. Dewitt, Y. Dori, Prevalence and cause of early Fontan complications: does the lymphatic circulation play a role? J. Am. Heart Assoc. 9 (2020) e015318.

[20] D.M. Biko, A.G. DeWitt, E.M. Pinto, R.E. Morrison, J.A. Johnstone, H. Griffis, M. L. O'Byrne, M.A. Fogel, M.A. Harris, S.L. Partington, K.K. Whitehead, D. Saul, D. J. Goldberg, J. Rychik, A.C. Glatz, M.J. Gillespie, J.J. Rome, Y. Dori, MRI evaluation of lymphatic abnormalities in the neck and thorax after Fontan surgery: relationship with outcome, Radiology 291 (2019) 774–780.

[21] B. Kelly, S. Mohanakumar, N. Telinius, M. Alstrup, V. Hjortdal, Function of upper extremity human lymphatics assessed by near-infrared fluorescence imaging, Lymphat. Res. Biol. 18 (2020) 226–231.

[22] S. Mohanakumar, B. Kelly, A.L.R. Turquetto, M. Alstrup, L.P. Amato, M.S. R. Barnabe, J.B.D. Silveira, F. Amaral, P.H. Manso, M.B. Jatene, V.E. Hjortdal, Functional lymphatic reserve capacity is depressed in patients with a Fontan circulation, Phys. Rep. 9 (2021) e14862.

[23] T. Hahn Rebecca, K. Lawlor Matthew, J. Davidson Charles, V. Badhwar, A. Sannino, E. Spitzer, P. Lurz, R. Lindman Brian, Y. Topilsky, J. Baron Suzanne, S. Chadderdon, K. Khalique Omar, H.L. Tang Gilbert, M. Taramasso, A. Grayburn Paul, L. Badano, J. Leipsic, J. Lindenfeld, S. Windecker, S. Vemulapalli, B. Redfors, C. Alu Maria, J. Cohen David, J. Rodés-Cabau, G. Ailawadi, M. Mack, O. Ben-Yehuda, B. Leon Martin, J. Hausleiter, S. Arnold, V. Bapat, N. Berry, P. Blanke, D. Burkhoff, M. Coylewright, N. Duggal, B. Galper, I. George, M. Guerrero, N. Hamid, V. Jagadeesan, S. Kodali, M. Krucoff, R. Lang, M. Madhavan, V. McLaughin, R. Mehran, F. Philippon, S. Sethi Sanjum, M. Simonato, R. Smith, N. Sodhi, J. Spertus, J. Stocker Thomas, G. Stone, Tricuspid valve academic research consortium definitions for tricuspid regurgitation and trial endpoints, J. Am. Coll. Cardiol. 82 (2023) 1711–1735.

[24] J.R. Levick, C.C. Michel, Microvascular fluid exchange and the revised Starling principle, Cardiovasc. Res. 87 (2010) 198–210.

[25] L. Asmarats, M. Taramasso, J. Rodés-Cabau, Tricuspid valve disease: diagnosis, prognosis and management of a rapidly evolving field, Nat. Rev. Cardiol. 16 (2019) 538–554.

[26] J.J. Silbiger, Atrial functional tricuspid regurgitation: an underappreciated cause of secondary tricuspid regurgitation, Echocardiography (Mount Kisco, NY). 36 (2019) 954–957.

[27] S.H. Patlolla, H.V. Schaff, R.A. Nishimura, J.M. Stulak, A.M. Chamberlain, S. V. Pislaru, V.T. Nkomo, Incidence and burden of tricuspid regurgitation in patients with atrial fibrillation, J. Am. Coll. Cardiol. 80 (2022) 2289–2298.

[28] M. Alkhouli, M.F. Eleid, R.A. Nishimura, C.S. Rihal, The role of invasive hemodynamics in guiding contemporary Transcatheter Valvular interventions, J. Am. Coll. Cardiol. Intv. 14 (2021) 2531–2544.

[29] M.H. Witte, A.E. Dumont, R.H. Clauss, B. Rader, N. Levine, E.S. Breed, Lymph circulation in congestive heart failure: effect of external thoracic duct drainage, Circulation 39 (1969) 723–733.

[30] R. Kristensen, B. Kelly, E. Kim, Y. Dori, V.E. Hjortdal, Lymphatic abnormalities on magnetic resonance imaging in single-ventricle congenital heart defects before Glenn operation, J. Am. Heart Assoc. 12 (2023) e029376.

[31] A. Vaikom House, D. David, J. Aguet, A.I. Dipchand, O. Honjo, E. Jean-St-Michel, M. Seed, S.J. Yoo, D.J. Barron, C.Z. Lam, Quantification of lymphatic burden in patients with Fontan circulation by T2 MR lymphangiography and associations with adverse Fontan status, Eur. Heart J. Cardiovasc. Imaging 24 (2023) 241–249.

[32] B. Ponikowska, J. Biegus, M. Fudim, G. Iwanek, M. Guzik, R. Przybylski, A. Szuba, A. Chachaj, R. Zymliński, Lower Extremity Lymphatic Flow/Drainage Assessment by Indocyanine Green Fluorescent Lymphography in Heart Failure Patients, JACC: Basic to Translational Science 9 (7) (2024) 906–917.

[33] M.B. Aldrich, J.C. Rasmussen, S.M. DeSnyder, W.A. Woodward, W. Chan, E. M. Sevick-Muraca, E.A. Mittendorf, B.D. Smith, M.C. Stauder, E.A. Strom, G. H. Perkins, K.E. Hoffman, M.P. Mitchell, C.H. Barcenas, L.E. Isales, S.F. Shaitelman, Prediction of breast cancer-related lymphedema by dermal backflow detected with near-infrared fluorescence lymphatic imaging, Breast Cancer Res. Treat. 195 (2022) 33–41.

[34] W.T. Abraham, M. Jonas, R.M. Dongaonkar, B. Geist, Y. Ueyama, K. Render, B. Youngblood, W. Muir, R. Hamlin, C.L. del Rio, Direct interstitial decongestion in an animal model of acute-on-chronic ischemic heart failure, JACC: Basic to Translational Science. 6 (2021) 872–881.

[35] Benjamin Kelly, Sheyanth Mohanakumar, Brooke Ford, Christopher L. Smith, Erin Pinto, David M. Biko, Vibeke E. Hjortdal, Yoav Dori, Sequential MRI Evaluation of Lymphatic Abnormalities over the Course of Fontan Completion, Radiology: Cardiothoracic Imaging 6 (3) (2024) e230315, https://doi.org/10.1148/ryct.230315.